ACS OMEGA

Open Access

http://pubs.acs.org/journal/acsodf

Article

Rapid Detection and Identification of Vancomycin-Sensitive Bacteria Using an Electrochemical Apta-Sensor

Zorica Novakovic, Majd Khalife, Vlad Costache, Maria Joao Camacho, Susana Cardoso, Veronica Martins, Ivana Gadjanski, Marko Radovic, and Jasmina Vidic*

Cite This: *ACS Omega* 2024, 9, 2841−2849

Read Online

ACCESS | Metrics & More | Article Recommendations | Supporting Information

ABSTRACT: In order to combat the complex and diverse infections caused by bacteria, it is essential to develop efficient diagnostic tools. Current techniques for bacterial detection rely on laborious multistep procedures, with high costs and extended time of analysis. To overcome these limitations, we propose here a novel portable electrochemical biosensor for the rapid detection and identification of Gram-positive bacteria that leverages the recognition capabilities of vancomycin and aptamers. A vancomycin-modified screen-printed carbon electrode was used to selectively capture Gram-positive bacteria susceptible to this antibiotic. Electrochemical impedance spectroscopy and scanning electron microscopy demonstrated that capture was achieved in 10 min, with a limit of detection of only 2 CFU/mL. We then tested the device's potential for aptamer-based bacterial identification using *Staphylococcus aureus* and *Bacillus cereus* as the test strains. Specifically, electrodes with captured bacteria were exposed to species-specific aptamers, and the resulting changes in current intensity were analyzed using differential pulse voltammetry. When used directly in untreated milk or serum, the system was able to successfully identify a small amount of *S. aureus* and *B. cereus* (100 CFU/mL) in less than 45 min. This novel biosensor has the potential to serve as an invaluable tool that could be used, even by inexperienced staff, in a broad range of settings including clinical diagnostics, food safety analysis, environmental monitoring, and security applications.

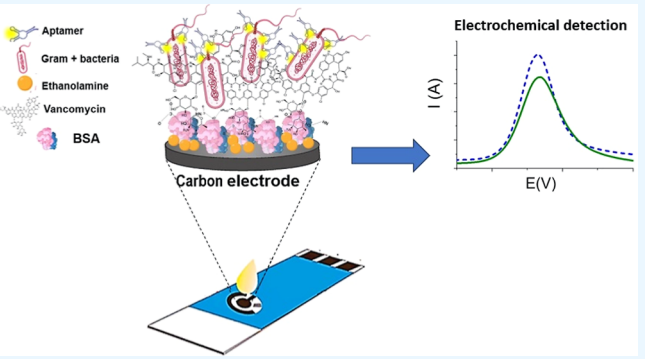

INTRODUCTION

Microbes have acquired resistance to all antibiotics currently in clinical use, and as a result, infectious diseases are again a major health concern.[1] Common bacterial infections are a leading cause of health loss, estimated to be linked to one in eight global deaths.[2] In 2019, the Gram-positive bacterium *Staphylococcus aureus* was associated with more than 1 million deaths globally.[2] *S. aureus* can cause a variety of diseases, ranging from minor tissue infections to chronic life-threatening deep-tissue conditions such as septic shock, pneumonia, osteomyelitis, and endocarditis. This bacterium is also a leading foodborne pathogen. Its aggressive pathogenicity derives at least in part from its production of numerous virulence factors, including cytolytic toxins and enzymes that degrade host tissues. Another Gram-positive bacterium of concern is *Bacillus cereus*, which is one of the leading etiological agents of toxin-induced foodborne diseases.[3−6] This pathogen is the second most significant agent responsible for collective foodborne poisoning in the European Union and China, and the fifth most common bacterial species linked with foodborne outbreaks in the USA, with an overall increasing trend in incidence.[5,7] Moreover, *B. cereus* can also cause serious nongastrointestinal pathologies, such as meningitis and pneumonia, with potentially fatal outcomes.[6] This species is widely present in the environment due to its ability to form resistant spores.[4] In general, but particularly with *S. aureus* and *B. cereus*, most bacterial infections are transmitted between people through cutaneous lesions or by consuming contaminated foods. In this context, the prevention and control of infectious disease are strongly dependent on the speed, sensitivity, and convenience of diagnosis, and new methods are sorely needed.

Currently, the main approaches for detecting bacterial pathogens rely on plate-counting and molecular techniques based on polymerase chain reactions (PCR) and enzyme-linked immunosorbent assays.[8−11] Instrument-based methods such as mass spectroscopy, infrared spectroscopy, flow cytometry, and sequencing enable sensitive and accurate bacterial detection. However, these methods are labor-intensive and expensive, necessitating the use of centralized

Received: October 19, 2023
Revised: November 23, 2023
Accepted: December 21, 2023
Published: January 4, 2024

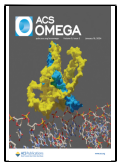

laboratories, trained personnel, and multiple steps of processing. Moreover, they are time-consuming, with turnaround times of up to 7 days, which limits their utility for on-site monitoring.[9,12] One promising approach that addresses these drawbacks is the use of biosensors. Modern biosensors are able to analyze small sample volumes using only a few processing steps and minimal sample preparation, making them highly practical options for simple on-site detection.[13,14]

Electrochemical biosensors, such as portable glucometers, are characterized by a high degree of sensitivity, selectivity, rapidity, and, importantly, low cost, and ease of miniaturization, making them excellent candidates for point-of-care diagnostics.[15−19] In particular, electrochemical biosensors based on screen-printed electrodes (SPEs), or other disposable electrodes that incorporate working, counter, and reference electrodes on one strip, are compact in design and thus highly convenient for on-site pathogen detection.[20−23] Among these, disposable screen-printed carbon electrodes (SPCEs) benefit from high electrical conductivity, enhanced stability, and efficient biofunctionalization, the latter due to the stable adsorption of a range of proteins, oligonucleotides, or polymers.[24] A number of microorganisms have been characterized using functionalized SPCEs, including *Escherichia coli*,[25,26] *Salmonella*,[27] *Pseudomonas aeruginosa*,[28] *S. aureus*,[29−31] and *Listeria*.[31,32] However, most of these electrochemical biosensors are designed to use specific antibodies, which presents several drawbacks in terms of limited storage stability, large size, and partial inhibition due to the matrix effect or their orientation on the electrode surface.[33,34] Significant efforts are thus underway to develop biorecognition elements that are smaller and more stable.

Particular attention has focused on vancomycin, a glycopeptide antibiotic known to form a five-point hydrogen bond with the terminal moieties D-alanyl-D-alanine (D-Ala-D-Ala) of peptidoglycans in cell walls, and which has shown high potential for capturing Gram-positive bacteria.[35−37] Vancomycin was first isolated from *Streptomyces orientalis* and is one of the oldest antibiotics, being in clinical use for more than 70 years. Vancomycin kills bacterial cells by inhibiting peptidoglycan cross-linking and therefore interrupting proper cell−wall synthesis in susceptible strains. However, this antibiotic has only a limited effect on Gram-negative bacteria because it cannot penetrate through the outer membrane that covers their cell wall. Vancomycin is very attractive for biosensor development because it is highly stable at room temperature[38] and contains a carboxylic functional group that provides a point for its covalent immobilization. Another alternative approach for biorecognition focuses on the use of DNA aptamers, which are characterized by high sensitivity and selectivity, and a lower cost than expensive antibodies.[15,16] In this case, binding to the target generally occurs as a function of the specific 3D shape of the aptamer. Many aptamers have been developed to bind whole bacterial cells,[39,40] including those of *S. aureus* and *B. cereus*.[41,42]

Here, we build upon previous research on the use of vancomycin-based electrochemical biosensors to detect Gram-positive bacteria by introducing specific aptamers that enable the identification of individual bacterial strains (Figure 1). In our system, the first recognition element was vancomycin conjugated to amine groups of an albumin-modified SPCE. When Gram-positive bacteria were present in the sample, their cells were captured by the antibiotic and then exposed to aptamers with specific affinity toward different bacterial strains.

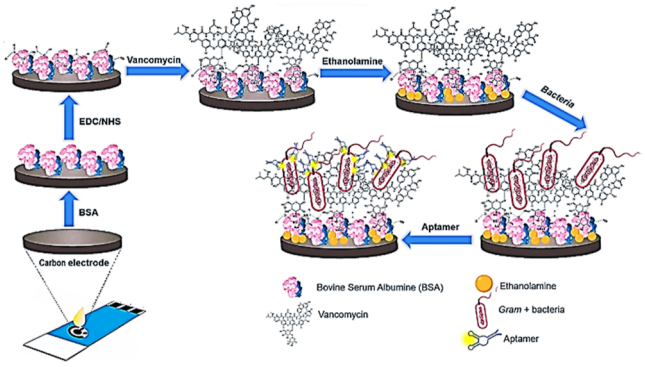

Figure 1. Schematic illustration of the principle for dual vancomycin/aptamer-based electrochemical bacterial detection and identification. A SPCE was modified by drop-casting with BSA. Vancomycin was attached to the surface by the EDC/NHS, and ethanolamine was used as a blocking agent. Bacterial suspension was added to the surface, incubated, and washed. The captured bacterial cells were identified by specific aptamers.

In this way, aptamers serve as a second recognition element that could be used to identify the strain of bacteria initially captured by vancomycin. Using these two recognition elements—vancomycin and aptamers—we developed an electrochemical sensor that can fully support rapid, sensitive, and strain-specific detection of Gram-positive bacteria directly in a biological matrix (milk and serum) at concentrations of only a few CFUs per mL.

EXPERIMENTAL SECTION

Materials and Reagents. Vancomycin hydrochloride, *N*-hydroxysuccinimide (NHS), *N*-[3-(dimethylamino)propyl]-*N*′-ethyl carbodiimide hydrochloride (EDC), potassium ferricyanide {$K_3[Fe(CN)_6]$}, potassium ferrocyanide {$K_4[Fe(CN)_6]$}, potassium chloride (KCl), and ethanolamine were purchased from Sigma-Aldrich (Saint Quentin Fallavier, France). Bovine serum albumin (BSA) was purchased from BioRad (Marnes-la-Coquette, France), and a stock solution of PBS (10x) was purchased from VWR Prolab (Rosny-sur-Bois, France). PBS at 1x was used in all experiments. SPCEs (model DropSens DRP-110) were purchased from DropSens (Metrohm, France). The electrode contains carbon graphite as working and counter electrodes, and a silver composite printed as a pseudoreference electrode over the same ceramic substrate. Powdered milk (Auchan, France) containing 36% protein, 52% lactose, and 0.8% fat (w/w) was purchased from a local supermarket and used to represent a real-world sample. Adult bovine serum was purchased from CliniSense (Nanterre, France). Aptamers were obtained from Eurofins Genomics SAS (Nantes, France). The specific anti-*S. aureus* aptamer (Apt1)[41] has the sequence 5′-TCC-CTA-CGG-CGC-TAA-CCC-CCC-CAG-TCC-GTC-CTC-CCA-GCC-TCA-CAC-CGC-CAC-CGT-GCT-ACA-AC-3′, and the specific anti-*B. cereus* aptamer (Sp14)[42] has the sequence 5′-AGC-AGC-ACA-GGG-TCA-GAT-GAT-ATG-TTT-ACG-CCA-GTG-GTA-TTA-TTG-GGG-TTG-ATA-TGT-CAC-CTA-TGC-GTG-3′. Stock solutions of aptamers (100 μM) were prepared using Milli-Q water and kept at −20 °C until use.

Bacterial Strains. The strains used in this study—*S. aureus* RN4220, *B. cereus* ATCC 14579, *E. coli* ATCC 14948, *Lactococcus lactis* MG1363, *Bacillus subtilis* BSB1, and *Staphylococcus carnosus* TM300—were cultured on brain-heart-

https://doi.org/10.1021/acsomega.3c08219
ACS Omega 2024, 9, 2841−2849

infusion (BHI) agar plates at 37 °C. A single colony was then transferred to a liquid BHI medium and grown at 37 °C overnight at 180 rpm until the saturation phase was reached. Bacterial dilutions (10^8 to 10^1 CFU/mL) were prepared in PBS. Quantitative bacterial counts were performed using the drop plate method for enumerating bacteria as described previously.[43]

Construction of Electrochemical Biosensor. The SPCE was functionalized with 2 mg/mL BSA at 4 °C for 18 h using the drop-casting method. Next, the working electrode was exposed to an activation reagent solution (40 mM EDC/10 mM NHS in 10 mM acetate buffer, pH 4.8) for 1 h at room temperature, rinsed with PBS, and functionalized with 1.5 mM vancomycin in PBS at room temperature for 1 h. The modified electrode was then washed with PBS. Finally, the remaining active sites in BSA were passivized with 50 mM ethanolamine at room temperature for 20 min and then rinsed with PBS.

Electrochemical Measurements. Electrochemical measurements were carried out using a potentiostat/galvanostat/impedance analyzer (PalmSens4, PalmSens BV, Netherlands) linked to a computer running PSTrace 5.8 software. All measurements were carried out in a solution containing 5 mM $K_3[Fe(CN)_6]/K_4[Fe(CN)_6]$ and 0.1 M KCl. Cyclic voltammetry (CV) was performed in the potential range from −0.2 to 1.2 V, with a scan rate of 0.5 V/s. Differential pulse voltammetry (DPV) was performed with a pulse amplitude of 0.025 V. Electrochemical impedance spectroscopy (EIS) measurements were performed over a frequency range from 1 Hz to 100 kHz, with a potential amplitude of 10 mV. The surface coverage, Γ, of the working electrode after BSA immobilization was calculated using the following equation

$$\mathrm{Ip} = \frac{n^2F^2A\nu\Gamma}{4RT} \quad (1)$$

where Ip is the Faradaic current, ν is the scan rate, A is the surface area of the electrode (4 mm^2), n is the number of electrons transferred, F is Faraday's constant, R is the molar gas constant, and T is the temperature.[44]

In order to extract specific electrical parameters representing different processes inside the electrochemical system, the EIS data were fitted with an equivalent circuit model. For this, the impedimetric measurements were calibrated with an equivalent circuit of the Randles cell provided by the software EIS Spectrum Analyzer (http://www.abc.chemistry.bsu.by/vi/analyser/), and the relevant electronic circuit elements were determined.[45]

Scanning Electron Microscopy. SPCEs were mounted on aluminum stubs (32 mm diameter) with carbon adhesive discs (Agar Scientific, Oxford Instruments SAS, Gomez-la-Ville, France) and visualized by field emission gun scanning electron microscopy (SEM FEG) as secondary-electron images (2 keV, spot size 30) under high-vacuum conditions with a Hitachi SU5000 instrument (Milexia, Saint-Aubin, France). Scanning electron microscopy (SEM) analyses were performed at the Microscopy and Imaging Platform MIMA2 (INRAE, Jouy-en-Josas, France) DOI: MIMA2, INRAE, 2018. Microscopy and Imaging Facility for Microbes, Animals and Foods.[46]

Detection in Milk and Serum. Overnight cultures of *S. aureus* and *B. cereus* were used to spike milk and adult bovine serum. A 1% milk solution was prepared by solubilizing powdered skim milk in a Milli-Q water. Bacterial cells, cultured in BHI, were collected by centrifugation and washed three times with PBS, and then 2 mL of bacterial suspension (10^8 CFU/mL) was added to 20 mL of milk or serum sample. These spiked samples were incubated at 37 °C under shaking for 1 h. After the incubation, each sample was diluted in PBS and tested electrochemically.

RESULTS AND DISCUSSION

Biosensor Fabrication and Characterization. The principle of the electrochemical method for bacterial detection is described in Figure 1.

First, the surface of the SPCE was functionalized with BSA by using the drop-casting method. Then, vancomycin was covalently attached to BSA, and nonoccupied sites were blocked with ethanolamine. Vancomycin binds to the cell wall of Gram-positive bacteria, which enables the capture of vancomycin-sensitive bacterial cells directly from contaminated samples without any pretreatment. Finally, strain-specific aptamers were used to identify the captured bacterial cells.

BSA was immobilized on the SPCE in a single drop-casting round, in which the protein (2 mg/mL) was pipetted on the bare working electrode. The immobilization parameters were optimized via evaluation of incubation volumes and surface coverage areas by using the ferro/ferricyanide redox couple and 0.1 KCl as the supporting electrolyte. CV using bare SPCE (black line) revealed a pair of well-defined and reversible redox peaks of the $[Fe(CN)_6]^{3-/4-}$, with high current intensities due to the excellent electron transfer of the used redox probe onto the carbon electrode surface (Figure S1a). A gradual decrease in current intensity was observed following electrode incubation with 2, 5, and 10 μL of BSA (Figure S1a). This reduction in current intensity is consistent with the fact that the charged proteins act as a barrier for electron transfer between the redox species and the electrode. The peak-to-peak separation indicated a satisfactory mass transfer at the electrode surface for all volumes tested. The highest surface coverage area, as calculated using eq 1, was obtained when the electrode was incubated with 10 μL of BSA (Γ ∼ 50%, Figure S1b). However, the immobilization of BSA should ideally be confined to the working electrode without any deposition onto the other electrodes. Thus, to avoid overspillage of BSA, 5 μL of BSA (providing a Γ of ∼35%) was used in further experiments. SEM of the working electrode area revealed that the randomly oriented micrometer carbon flakes were uniformly covered with small spherical particles after immobilization using this volume of BSA (Figure 2a,b).

The BSA-carbon surface was further functionalized with vancomycin using EDC/NHS cross-linking reagents. EDC, as a zero-length cross-linking agent, was used to couple the carboxyl group of vancomycin to the primary amines of BSA, while NHS was employed to increase the stability of the active ester. Figures S2 and S3 depict the process of optimization of both vancomycin concentration and incubation time, as evaluated using the DPV technique and ferro-/ferricyanide with KCl. The voltammograms of the surface before and after vancomycin immobilization were similar, but the current intensities were smaller after antibiotic immobilization, indicating that the vancomycin layer had a blocking effect on the electroactive surface. The smallest peak currents were obtained with 1.5 mM vancomycin and 60 min of incubation time, so these parameters were selected for further experiments. Successful vancomycin loading under these conditions was confirmed by SEM as bright dots on the working electrode surface (Figure 2c). The observed dots were μm in size, suggesting a partial aggregation of vancomycin.

https://doi.org/10.1021/acsomega.3c08219
ACS Omega 2024, 9, 2841−2849

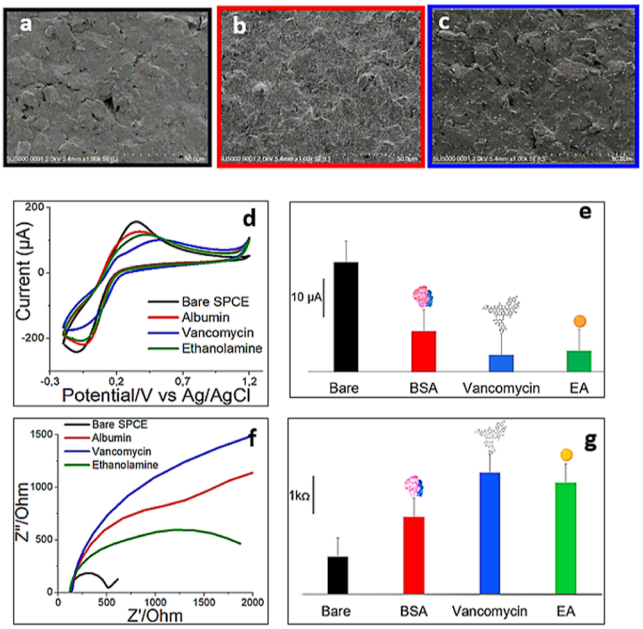

Figure 2. Electrode functionalization. SEM images (a) before and (b) after incubation with BSA and (c) BSA + vancomycin. (d) CVs of 5 mM $K_3[Fe(CN)_6]/K_4[Fe(CN)_6]$ with 0.1 M KCl using a bare electrode or an electrode functionalized with BSA, BSA/vancomycin, and BSA/vancomycin/ethanolamine. (e) Current variations for each functionalization step. Bars stand for the peak current changes after each step of functionalization. (f) Nyquist plots of impedance spectra obtained from bare SPCE and SPCE modified with BSA, BSA/vancomycin, and BSA/vancomycin/ethanolamine. (g) Fitting values of the charge transfer resistance, R_{ct}, after each step of SPCE functionalization. CV parameters: potential range from −0.2 to 1.2 V, scan rates 0.5 V/s. EIS parameters: frequencies ranged from 1 to 100 Hz, amplitude 10 mV.

CV and EIS were used to characterize the layer-by-layer functionalization of the working electrode under the optimized conditions. Measurements were carried out on the corresponding electrodes in a solution containing ferro- and fluorocyanide and KCl. As shown in Figure 2d, the well-defined and reversible redox peaks for $[Fe(CN)_6]^{3-/4-}$ decreased in intensity after the immobilization of BSA and vancomycin, confirming electrode functionalization. However, after the blocking step with ethanolamine, an increase in the voltammetric response of the electrode was observed (Figure 2d,e). This slight increase in the current response was probably due to a reorganization of immobilized molecules during blocking that then enhanced the electron transfer of $[Fe(CN)_6]^{3-/4-}$. Indeed, it was previously suggested that noncovalently bound proteins may be displaced by the small molecule of ethanolamine.[47] EIS monitoring of electrode functionalization revealed a notable increase in the diameter of semicircles in the Nyquist diagrams after the first two steps of biosensor construction and a decrease after the surface blocking step, which is consistent with the formation of different layers on the carbon electrode surface (Figure 2f,g). When the EIS curves were fitted with the equivalent circuit, the results suggested that the immobilization of BSA and vancomycin on the SPCE reduced the penetration of the redox probe and accordingly increased the charge transfer resistance (R_{ct}) (Figure 2g). Instead, blocking the BSA-active esters with ethanolamine promoted redox probe transfer to the electrode surface, with a resulting decrease in R_{ct}. The stability of functionalized electrodes was assessed by CV in a solution of the $[Fe(CN)_6]^{3-/4-}$ redox couple with 0.1 KCl (Figure S4). After one cycle, a stable biosensor response was obtained, so the same method of electrode preparation was used for all future measurements.

Biosensor Responses toward Vancomycin-Sensitive Bacteria. The vancomycin-modified SPCE was then tested using a panel of bacteria at various concentrations (Figures 3 and S4). Bacterial binding to the electrode surface was directly detected using EIS, without labeling or sample pretreatment.[20,35,36] The binding of Gram-positive bacteria to the electrode carrying vancomycin increased the impedance spectra at all frequencies studied (Figures 3a and S5). In contrast, the introduction of Gram-negative *E. coli* resulted in no changes to Nyquist plots of impedance spectra, even at high bacterial concentrations of 10^7 to 10^9 CFU/mL (Figure 3c). These data strongly suggested that this electrode can distinguish between vancomycin-sensitive and vancomycin-resistant bacterial strains. The equivalent circuit (inserts in Figures 3a and S5) was found to adequately fit the data over the entire frequency range. The circuit included the following elements: R_1, the internal resistance of the electrolyte solution, which together with the parallel connected capacitance, C_1, reflects the nonhomogeneity in the surface layer; R_2, the resistance caused by electrochemical reactions that occur at the electrode surface, including charge transfer between the electrode and the electrolyte; R_3 (charge transfer resistance, R_{ct}) and C_2 inside the third circuit, which define the modification due to bacterial capture on the electrode surface; and W_1, the Warburg resistance associated with the low-frequency region of the spectrum, displayed as a tilted line and reflecting a diffusion process occurring at the electrode−electrolyte interface. When bacterial cells attach to the surface of the electrode, they effectively reduce the area of the electrode that the current reaches and thereby increase the interface resistance.

For all Gram-positive bacteria tested, we found a systematic increase in R_{ct} (R_3, represented by the width of the semicircle in the Nyquist plot) with increasing bacterial concentrations, indicating a loss in the efficiency of the mass transfer phenomenon and/or a difference in the dielectric or conductive properties as a result of the bacteria captured on the electrode surface. Instead, the value of the solution resistance, R_1, remained practically constant (Table S1). Because of its sensitivity to variations in the bacterial concentration, R_{ct} was selected as the relevant parameter for bacterial quantification in further analyses. Indeed, when the electrode was incubated with *B. cereus* and *S. aureus* in concentrations between 10^2 and 10^9 CFU/mL, we observed a linear increase in R_{ct}, with correlation coefficients (R^2) of 0.98 and 0.96, respectively (Figure 3a,b, right panels). Limits of detection (LoD) were calculated using 3 s/m criteria, where 's' is the standard deviation of the blank solution (buffer containing no bacteria) and 'm' is the slope of the linear calibration curves in Figure 3a,b (right panels); this produced values of 2.4 CFU/mL and 2.7 CFU/mL for *B. cereus* and *S. aureus*, respectively. Finally, we assessed the reproducibility of responses and obtained a relative standard deviation (RSD) of 13%, which demonstrated the satisfactory performance of this proof-of-concept approach. Figure S5 depicts EIS responses and the corresponding calibration curves obtained for the other Gram-positive bacteria tested, i.e., *B. subtilis*, *S. carnosus*, and *L. lactis*, together with the corresponding analytical

https://doi.org/10.1021/acsomega.3c08219
ACS Omega 2024, 9, 2841−2849

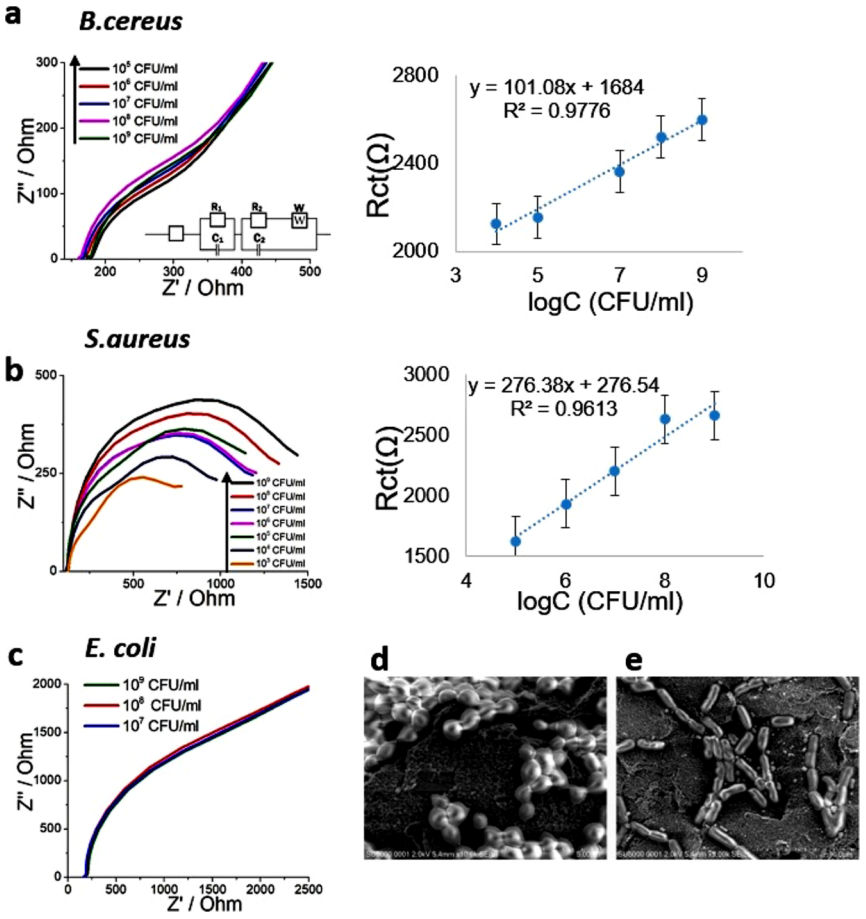

Figure 3. Bacterial detection using a vancomycin-modified electrode. (a) EIS Nyquist plots obtained using increasing amounts of *B. cereus* cells, with the equivalent electrical circuit applied to fit the Nyquist plot in insert. The circuit included the following: R_1, the internal resistance of the electrolyte solution; C_1, the constant phase element; R_2, the resistance due to electrochemical reactions; R_3, the charge transfer resistance; C_2, the capacitance due to bacterial capture on the electrode surface; and W_1, the Warburg resistance. The calibration curve was obtained by using the R_{ct} component of the EIS equivalent circuit. All data points represent the mean ± SD of three independent experiments. (b) EIS Nyquist plots and calibration curve for *S. aureus*. (c) EIS Nyquist plots for *E. coli*. (d) SEM images of electrodes after incubation with *S. carnosus* or (e) *B. cereus*. Scale bar, 5 μm.

parameters. Figure 3d,e displays SEM micrographs of cells of *S. carnosus* and *B. cereus*, respectively, attached to a vancomycin-functionalized SPCE electrode. In contrast, when *E. coli* was incubated with the functionalized electrode only salt crystals were observed on the surface confirming the absence of the bacterium adherence (Figure S6). Overall, these data demonstrate that the electrochemical biosensor we developed enabled the reliable and sensitive detection of Gram-positive bacteria. However, at this point, it was not possible to distinguish between different vancomycin-sensitive strains.

Optimization of Bacterial Identification. Using the cell-SELEX procedure, it is possible to select aptamers that recognize cell surface epitopes and can thus be used for bacterial detection without the need for complicated sample preparation, lysing of bacterial cells, or biomarker purification.[48,49] We wanted to test whether these aptamers could be coupled to our vancomycin-based sensing platform for the quantification and identification of Gram-positive bacteria. For this, we used the previously validated aptamers Sp14, selected to bind to cells of *B. cereus*,[42] and Apt1, selected to bind to cells of *S. aureus*.[41,50] To optimize aptamer concentrations, electrodes carrying captured bacteria were incubated with different concentrations of Apt1 or Sp14, intensively washed, and characterized by using DPV (Figure 4). We used DPV for bacterial identification to achieve higher sensitivity compared to CV. When Sp14 or Apt1 was incubated with the functionalized electrode carrying no bacterial cells, no modification was detected in the peak of $[Fe(CN)_6]^{3-/4-}$ at 0.15 V versus Ag/AgCl (Figure S7). Moreover, no change in peak current (ΔI) was observed when the electrode with captured *B. cereus* cells (10^4 CFU/mL) was incubated with Apt1, or when the electrode with captured *S. aureus* (10^4 CFU/mL) was incubated with Sp14 (Figure 4). In contrast, when the electrodes with immobilized bacteria were incubated with their corresponding aptamer, i.e., *B. cereus* with Sp14 and *S. aureus* with Apt1, there was a notable reduction in the peak intensity (Figure 4a,b). Keeping the concentration of the bacterial sample constant (10^4 CFU/mL), we tested different concentrations of Sp14 and Apt1 (0.1, 1, and 10 μM) to determine the optimized dosage for each aptamer. For Apt 1, DPV analysis revealed that the reduction in peak intensity continued to increase with increasing concentrations, while for Sp14, the maximal reduction in peak intensity was obtained with 1 μM Sp14 (Figure 4a,b). Therefore, the next set of measurements was carried out using aptamer concentrations of 10 μM Apt1 and 1 μM Sp14. This difference in optimal concentration may arise due to steric and electrostatic repulsion between the negatively charged aptamers.[51]

https://doi.org/10.1021/acsomega.3c08219
ACS Omega 2024, 9, 2841−2849

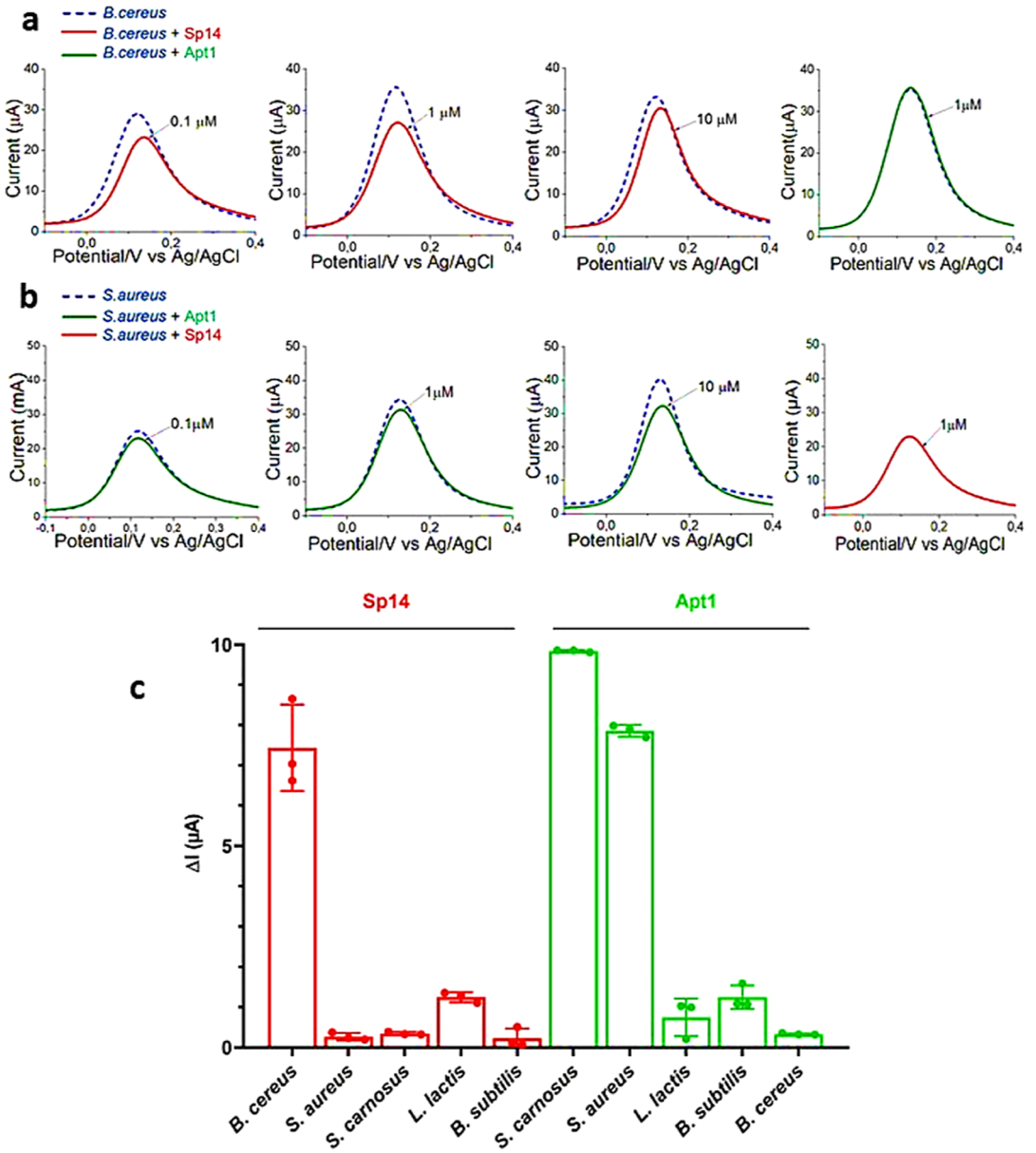

Figure 4. Identification of captured bacterial cells. Optimization of the apta-assay was performed with different concentrations of specific aptamers. Specificity was tested using control bacterial strains. (a) DPVs obtained after electrodes carrying *B. cereus* (10^4 CFU/mL) cells were incubated with the aptamers Sp14 (specific for *B. cereus*) or Apt1 (specific for *S. aureus*). (b) DPVs obtained for electrodes carrying *S. aureus* (10^4 CFU/mL) after incubation with Sp14 or Apt1. (c) Specificity study for the apta-assay performed in PBS inoculated with various bacteria. For these assays, 1 μM Sp14 or 10 μM Apt1 and 10^8 CFU/mL of all strains were used. The error bars show standard deviation for $n = 3$. DPV parameters: potential ranged from −0.2 to 0.5 V, pulse amplitude 0.025 V.

To assess the specificity of the developed assay, the two aptamers were further tested using high concentrations of other Gram-positive strains (10^8 CFU/mL) in PBS. As shown in Figure 4c, the difference in current intensities obtained before and after the addition of an aptamer was generally 6- to 9-fold higher with the target bacterium (*B. cereus* or *S. aureus*) than when tested with nontarget bacteria. The one exception to this was found with Apt1, which provided high current responses with both *S. aureus* and *S. carnosus*. This cross-reactivity is likely the result of similarity in the Apt1-specific cell surface epitopes between the two congeneric bacterial strains, both belonging to the genus *Staphylococcus*.

Detection of *S. aureus* and *B. cereus* in Milk Samples and Adult Bovine Serum. To demonstrate the potential practical applications of the developed biosensor, we conducted proof-of-concept experiments that modeled bacterial detection in cases of food contamination and sepsis. Cow milk and serum were selected as model biological fluids because they both are extremely complex and can be naturally contaminated by both *S. aureus* and *B. cereus*. When serum or milk samples with no bacterial cells were incubated together with the vancomycin-modified electrode, we observed no variation in signals (Figure S8). We then spiked samples with three different bacterial concentrations (10^2, 10^3, and 10^4 CFU/mL), recorded DPV before and after aptamer addition, and calculated the resulting ΔI. The mean value, standard deviation, and coefficient of variation of each parameter were

https://doi.org/10.1021/acsomega.3c08219
ACS Omega 2024, 9, 2841−2849

calculated for each of the three different concentrations of the two target bacteria (Table 1).

Table 1. Reproducibility Assays of the Apta-Sensor in Serum and Milk[a]

	serum			milk		
B. cereus	ΔI (μA)	S.D.	c.v. (%)	ΔI	S.D.	c.v. (%)
10^4 CFU/mL	8.8	±1.3	11	25.2	±1.4	5.5
10^3 CFU/mL	6.1	±0.7	11	5.84	±0.18	3
10^2 CFU/mL	5.3	±0.3	15		±0.21	10.1
	serum			milk		
S. aureus	ΔI (μA)	S.D.	c.v. (%)	ΔI	S.D.	c.v. (%)
10^4 CFU/mL	5.9	±1.9	5	16.9	±1.6	9
10^3 CFU/mL	4.5	±0.5	11	3.9	±0.35	9
10^2 CFU/mL	2.4	±0.4	16	2	±0.12	6

[a]ΔI, reduction in peak intensity after aptamer addition. S.D., standard deviation. c.v., coefficient of variation (%).

The results demonstrated that the sensor was sensitive enough to identify captured bacteria at concentrations as low as 1×10^2 CFU/mL. Mean coefficients of variation were less than 10% of RSD, indicating that the results of this novel bacterial sensor were highly reproducible. Moreover, this experiment illustrates that the analytical method used here can be applied directly in complex matrices, greatly increasing the possibilities for rapid, reliable, and portable bacterial identification.

CONCLUSIONS

In this work, we used vancomycin-modified SPCEs to create the first electrochemical aptasensor capable of both detecting and identifying Gram-positive bacteria. Vancomycin reacts with the accessible peptidoglycan moieties D-Ala-D-Ala in the cell walls of Gram-positive bacteria; deposition of this antibiotic on the albumin-modified working carbon electrode creates a biorecognition receptor that strongly binds sensitive bacteria, thus enabling extreme acceleration of the detection procedure. The electrochemical performance of the vancomycin-modified electrode was investigated using a simple and rapid protocol that evaluated bacterial detection based on faradic impedance. Charge transfer resistance was selected as the best parameter with which to assess bacterial capture of the electrode. We found that the change in R_{ct} varied linearly with the concentration of vancomycin-sensitive bacteria (*S. aureus*, *B. cereus*, *B. subtilis*, *S. carnosus*, and *L. lactis*), with a low detection limit (only a few CFUs per mL), while no variation in R_{ct} was observed with vancomycin-resistant *E. coli*. Through the addition of a single extra step involving a 30 min incubation of the captured bacteria with a strain-specific aptamer, we created a dual recognition system that was not only able to detect vancomycin-sensitive bacteria but could also identify the individual bacterial species present. When we tested the sensor's performance on *B. cereus* and *S. aureus* in milk and serum using DPV, we found that detection and identification of the target bacteria were highly reproducible and could be accomplished with a total assay time of less than 45 min. This novel dual-recognition strategy presents considerable advantages over traditional culture-based methods: using a simple and rapid protocol, it can quantitatively analyze bacterial strains in a variety of settings, making this technology highly promising for point-of-care applications in fields such as food safety, human and animal health, and environmental monitoring.

ASSOCIATED CONTENT

Supporting Information

The Supporting Information is available free of charge at https://pubs.acs.org/doi/10.1021/acsomega.3c08219.

Optimization of BSA immobilization; optimization of vancomycin immobilization; bacterial detection using vancomycin-modified carbon SPE; background signals; and fitting values of the equivalent circuit elements for Gram-positive bacteria (PDF)

AUTHOR INFORMATION

Corresponding Author

Jasmina Vidic − *Université Paris-Saclay, INRAE, AgroParisTech, Micalis Institute, 78350 Jouy-en-Josas, France*; orcid.org/0000-0002-8549-8199; Email: jasmina.vidic@inrae.fr

Authors

Zorica Novakovic − *University of Novi Sad, BioSense Institute, 21000 Novi Sad, Serbia*

Majd Khalife − *Université Paris-Saclay, INRAE, AgroParisTech, Micalis Institute, 78350 Jouy-en-Josas, France*

Vlad Costache − *Université Paris-Saclay, INRAE, AgroParisTech, Micalis Institute, 78350 Jouy-en-Josas, France; MIMA2 Imaging Core Facility, Microscopie et Imagerie des Microorganismes, Animaux et Aliments, INRAE, 78350 Jouy-en-Josas, France*

Maria Joao Camacho − *INESC Microsistemas e Nanotecnologias Rua Alves Redol, 1000-049 Lisbon, Portugal*

Susana Cardoso − *INESC Microsistemas e Nanotecnologias Rua Alves Redol, 1000-049 Lisbon, Portugal*; orcid.org/0000-0001-6913-6529

Veronica Martins − *INESC Microsistemas e Nanotecnologias Rua Alves Redol, 1000-049 Lisbon, Portugal*

Ivana Gadjanski − *University of Novi Sad, BioSense Institute, 21000 Novi Sad, Serbia*; orcid.org/0000-0003-0713-7897

Marko Radovic − *University of Novi Sad, BioSense Institute, 21000 Novi Sad, Serbia*; orcid.org/0000-0001-7565-4015

Complete contact information is available at: https://pubs.acs.org/10.1021/acsomega.3c08219

Author Contributions

Z.N., M. K., M.J.C., and V. C. performed experiments. I.G., J.V., S.C., M. R., and V. M. contributed to funding acquisition and project administration. J.V. designed and supervised research and wrote the paper. All authors reviewed the manuscript and have given approval to its final version.

Notes

The authors declare no competing financial interest.

ACKNOWLEDGMENTS

This work was supported in part by the IPANEMA project, which received funding from the European Union's Horizon 2020 research and innovation program under grant agreement No 872662 and the bilateral Franco-Portugal project PHC−PESSAO 2022 (No 44613UG), and in part by the French

National Agency for Research (ANR-21-CE42 ELISE projects, to J.V.). M.J.C. acknowledges funding from the Fundação para a Ciencia e Tecnologia (FCT) through the grant SFRH/BD/138724/2018.

REFERENCES

(1) Darby, E. M.; Trampari, E.; Siasat, P.; Gaya, M. S.; Alav, I.; Webber, M. A.; Blair, J. M. Molecular mechanisms of antibiotic resistance revisited. *Nat. Rev. Microbiol.* **2023**, *21* (5), 280−295.
(2) Ikuta, K. S.; Swetschinski, L. R.; Robles Aguilar, G.; Sharara, F.; Mestrovic, T.; Gray, A. P.; Davis Weaver, N.; Wool, E. E.; Han, C.; Gershberg Hayoon, A.; et al. Global mortality associated with 33 bacterial pathogens in 2019: a systematic analysis for the Global Burden of Disease Study 2019. *Lancet* **2022**, *400* (10369), 2221−2248.
(3) Jovanovic, J.; Ornelis, V. F.; Madder, A.; Rajkovic, A. Bacillus cereus food intoxication and toxicoinfection. *Compr. Rev. Food Sci. Food Saf.* **2021**, *20* (4), 3719−3761.
(4) Vidic, J.; Chaix, C.; Manzano, M.; Heyndrickx, M. Food Sensing: Detection of Bacillus cereus Spores in Dairy Products. *Biosensors* **2020**, *10* (3), 15.
(5) Ramarao, N.; Tran, S.-L.; Marin, M.; Vidic, J. Advanced Methods for Detection of Bacillus cereus and Its Pathogenic Factors. *Sensors* **2020**, *20* (9), 2667.
(6) Cormontagne, D.; Rigourd, V.; Vidic, J.; Rizzotto, F.; Bille, E.; Ramarao, N. Bacillus cereus induces severe infections in preterm neonates: implication at the hospital and human milk bank level. *Toxins* **2021**, *13* (2), 123.
(7) Zhu, K.; Hölzel, C. S.; Cui, Y.; Mayer, R.; Wang, Y.; Dietrich, R.; Didier, A.; Bassitta, R.; Märtlbauer, E.; Ding, S. Probiotic Bacillus cereus strains, a potential risk for public health in China. *Front. Microbiol.* **2016**, *7*, 718.
(8) Kotsiri, Z.; Vidic, J.; Vantarakis, A. Applications of biosensors for bacteria and virus detection in food and water-A systematic review. *J. Environ. Sci.* **2022**, *111*, 367−379.
(9) Vidic, J.; Manzano, M.; Chang, C.-M.; Jaffrezic-Renault, N. Advanced biosensors for detection of pathogens related to livestock and poultry. *Vet. Res.* **2017**, *48* (1), 11−22.
(10) Balbinot, S.; Srivastav, A. M.; Vidic, J.; Abdulhalim, I.; Manzano, M. Plasmonic biosensors for food control. *Trends Food Sci. Technol.* **2021**, *111*, 128−140.
(11) Vidic, J.; Vizzini, P.; Manzano, M.; Kavanaugh, D.; Ramarao, N.; Zivkovic, M.; Radonic, V.; Knezevic, N.; Giouroudi, I.; Gadjanski, I. Point-of-need DNA testing for detection of foodborne pathogenic bacteria. *Sensors* **2019**, *19* (5), 1100.
(12) Mazur, F.; Tjandra, A. D.; Zhou, Y.; Gao, Y.; Chandrawati, R. Paper-based sensors for bacteria detection. *Nat. Rev. Bioeng.* **2023**, *1* (3), 180−192.
(13) Martins, S. A.; Martins, V. C.; Cardoso, F. A.; Germano, J.; Rodrigues, M.; Duarte, C.; Bexiga, R.; Cardoso, S.; Freitas, P. P. Biosensors for on-farm diagnosis of mastitis. *Front. Bioeng. Biotechnol.* **2019**, *7*, 186.
(14) Soares, A. R.; Afonso, R.; Martins, V.; Palos, C.; Pereira, P.; Caetano, D. M.; Carta, D.; Cardoso, S. On-site magnetic screening tool for rapid detection of hospital bacterial infections: Clinical study with Klebsiella pneumoniae cells. *Biosens. Bioelectron.: X* **2022**, *11*, 100149.
(15) Vidic, J.; Manzano, M. Electrochemical biosensors for rapid pathogen detection. *Curr. Opin. Electrochem.* **2021**, *29*, 100750.
(16) Bobrinetskiy, I.; Radovic, M.; Rizzotto, F.; Vizzini, P.; Jaric, S.; Pavlovic, Z.; Radonic, V.; Nikolic, M. V.; Vidic, J. Advances in nanomaterials-based electrochemical biosensors for foodborne pathogen detection. *Nanomaterials* **2021**, *11* (10), 2700.
(17) Dincer, C.; Bruch, R.; Costa-Rama, E.; Fernández-Abedul, M. T.; Merkoçi, A.; Manz, A.; Urban, G. A.; Güder, F. Disposable sensors in diagnostics, food, and environmental monitoring. *Adv. Mater.* **2019**, *31* (30), 1806739.
(18) Cho, I.-H.; Kim, D. H.; Park, S. Electrochemical biosensors: Perspective on functional nanomaterials for on-site analysis. *Biomater. Res.* **2020**, *24* (1), 6.
(19) Vizzini, P.; Braidot, M.; Vidic, J.; Manzano, M. Electrochemical and Optical Biosensors for the Detection of Campylobacter and Listeria: An Update Look. *Micromachines* **2019**, *10* (8), 500.
(20) Podunavac, I.; Kukkar, M.; Léguillier, V.; Rizzotto, F.; Pavlovic, Z.; Janjušević, L.; Costache, V.; Radonic, V.; Vidic, J. Low-cost goldleaf electrode as a platform for Escherichia coli immunodetection. *Talanta* **2023**, *259*, 124557.
(21) Taleat, Z.; Khoshroo, A.; Mazloum-Ardakani, M. Screen-printed electrodes for biosensing: A review (2008−2013). *Microchim. Acta* **2014**, *181*, 865−891.
(22) Moya, A.; Gabriel, G.; Villa, R.; Javier del Campo, F. Inkjet-printed electrochemical sensors. *Curr. Opin. Electrochem.* **2017**, *3* (1), 29−39.
(23) Moro, G.; Bottari, F.; Van Loon, J.; Du Bois, E.; De Wael, K.; Moretto, L. M. Disposable electrodes from waste materials and renewable sources for (bio) electroanalytical applications. *Biosens. Bioelectron.* **2019**, *146*, 111758.
(24) Arduini, F.; Micheli, L.; Moscone, D.; Palleschi, G.; Piermarini, S.; Ricci, F.; Volpe, G. Electrochemical biosensors based on nanomodified screen-printed electrodes: Recent applications in clinical analysis. *Trac. Trends Anal. Chem.* **2016**, *79*, 114−126.
(25) Lin, Y.-H.; Chen, S.-H.; Chuang, Y.-C.; Lu, Y.-C.; Shen, T. Y.; Chang, C. A.; Lin, C.-S. Disposable amperometric immunosensing strips fabricated by Au nanoparticles-modified screen-printed carbon electrodes for the detection of foodborne pathogen Escherichia coli O157: H7. *Biosens. Bioelectron.* **2008**, *23* (12), 1832−1837.
(26) Shoaie, N.; Forouzandeh, M.; Omidfar, K. Voltammetric determination of the Escherichia coli DNA using a screen-printed carbon electrode modified with polyaniline and gold nanoparticles. *Microchim. Acta* **2018**, *185*, 217.
(27) Ren, Y.; Ji, J.; Sun, J.; Pi, F.; Zhang, Y.; Sun, X. Rapid detection of antibiotic resistance in Salmonella with screen printed carbon electrodes. *J. Solid State Electrochem.* **2020**, *24*, 1539−1549.
(28) Rashid, J. I. A.; Kannan, V.; Ahmad, M. H.; Mon, A. A.; Taufik, S.; Miskon, A.; Ong, K. K.; Yusof, N. A. An electrochemical sensor based on gold nanoparticles-functionalized reduced graphene oxide screen printed electrode for the detection of pyocyanin biomarker in Pseudomonas aeruginosa infection. *Mater. Sci. Eng., C* **2021**, *120*, 111625.
(29) Ghalkhani, M.; Sohouli, E.; Khaloo, S. S.; Vaziri, M. H. Architecting of an aptasensor for the staphylococcus aureus analysis by modification of the screen-printed carbon electrode with aptamer/Ag-Cs-Gr QDs/NTiO2. *Chemosphere* **2022**, *293*, 133597.
(30) Khue, V. Q.; Huy, T. Q.; Phan, V. N.; Tuan-Le, A.; Thanh Le, D. T.; Tonezzer, M.; Hong Hanh, N. T. Electrochemical stability of screen-printed electrodes modified with Au nanoparticles for detection of methicillin-resistant Staphylococcus aureus. *Mater. Chem. Phys.* **2020**, *255*, 123562.
(31) Eissa, S.; Zourob, M. Ultrasensitive peptide-based multiplexed electrochemical biosensor for the simultaneous detection of Listeria monocytogenes and Staphylococcus aureus. *Microchim. Acta* **2020**, *187*, 486−511.
(32) Jampasa, S.; Ngamrojanavanich, N.; Rengpipat, S.; Chailapakul, O.; Kalcher, K.; Chaiyo, S. Ultrasensitive electrochemiluminescence sensor based on nitrogen-decorated carbon dots for Listeria monocytogenes determination using a screen-printed carbon electrode. *Biosens. Bioelectron.* **2021**, *188*, 113323.
(33) Duarte, C.; Costa, T.; Carneiro, C.; Soares, R.; Jitariu, A.; Cardoso, S.; Piedade, M.; Bexiga, R.; Freitas, P. Semi-quantitative method for streptococci magnetic detection in raw milk. *Biosensors* **2016**, *6* (2), 19.
(34) Duarte, C. M.; Carneiro, C.; Cardoso, S.; Freitas, P. P.; Bexiga, R. Semi-quantitative method for Staphylococci magnetic detection in raw milk. *J. Dairy Res.* **2017**, *84* (1), 80−88.
(35) Yang, Z.; Wang, Y.; Zhang, D. A novel multifunctional electrochemical platform for simultaneous detection, elimination, and

https://doi.org/10.1021/acsomega.3c08219
ACS Omega 2024, 9, 2841−2849

inactivation of pathogenic bacteria based on the Vancomycin-functionalised AgNPs/3D-ZnO nanorod arrays. *Biosens. Bioelectron.* **2017**, *98*, 248−253.
(36) Norouz Dizaji, A.; Ali, Z.; Ghorbanpoor, H.; Ozturk, Y.; Akcakoca, I.; Avci, H.; Dogan Guzel, F. Electrochemical-based "antibiotsensor"for the whole-cell detection of the vancomycin-susceptible bacteria. *Talanta* **2021**, *234*, 122695.
(37) Hu, W.-C.; Pang, J.; Biswas, S.; Wang, K.; Wang, C.; Xia, X.-H. Ultrasensitive detection of bacteria using a 2D MOF nanozyme-amplified electrochemical detector. *Anal. Chem.* **2021**, *93* (24), 8544−8552.
(38) Ensom, M. H.; Decarie, D.; Lakhani, A. Stability of Vancomycin 25 mg/mL in Ora-Sweet and Water in Unit-Dose Cups and Plastic Bottles at 4°C and 25°C. *Can. J. Hosp. Pharm.* **2010**, *63* (5), 366.
(39) Deb, A.; Gogoi, M.; Mandal, T. K.; Sinha, S.; Pattader, P. S. G. Specific Instantaneous Detection of Klebsiella pneumoniae for UTI Diagnosis with a Plasmonic Gold Nanoparticle Conjugated Aptasensor. *ACS Appl. Bio Mater.* **2023**, *6* (8), 3309−3318.
(40) Ferrer-Vilanova, A.; Alonso, Y.; J Ezenarro, J.; Santiago, S.; Muñoz-Berbel, X.; Guirado, G. Electrochromogenic Detection of Live Bacteria Using Soluble and Insoluble Prussian Blue. *ACS Omega* **2021**, *6* (46), 30989−30997.
(41) Abbaspour, A.; Norouz-Sarvestani, F.; Noori, A.; Soltani, N. Aptamer-conjugated silver nanoparticles for electrochemical dual-aptamer-based sandwich detection of staphylococcus aureus. *Biosens. Bioelectron.* **2015**, *68*, 149−155.
(42) Zhouping, W.; Huihui, Y.; Yu, X.; Nuo, D. Oligonucleotide aptamer set for specifically identifying Bacillus cereus. CN104694646B, 2015.
(43) Kotsiri, Z.; Vantarakis, A.; Rizzotto, F.; Kavanaugh, D.; Ramarao, N.; Vidic, J. Sensitive Detection of E. coli in Artificial Seawater by Aptamer-Coated Magnetic Beads and Direct PCR. *Appl. Sci.* **2019**, *9* (24), 5392.
(44) Eckermann, A. L.; Feld, D. J.; Shaw, J. A.; Meade, T. J. Electrochemistry of redox-active self-assembled monolayers. *Coord. Chem. Rev.* **2010**, *254* (15−16), 1769−1802.
(45) Bondarenko, A.; Ragoisha, G. *Progress In Chemometrics Research*; Nova Science Publishers: New York, 2005, pp 89−102.
(46) INRAE *Microscopie et Imagerie des Micro-Organismes Animaux et Aliments*. 2022.
(47) Escamilla-Gómez, V.; Campuzano, S.; Pedrero, M.; Pingarrón, J. M. Gold screen-printed-based impedimetric immunobiosensors for direct and sensitive Escherichia coli quantisation. *Biosens. Bioelectron.* **2009**, *24* (11), 3365−3371.
(48) Duan, Y.; Zhang, C.; Wang, Y.; Chen, G. Research progress of whole-cell-SELEX selection and the application of cell-targeting aptamer. *Mol. Biol. Rep.* **2022**, *49* (8), 7979−7993.
(49) Rizzotto, F.; Khalife, M.; Hou, Y.; Chaix, C.; Lagarde, F.; Scaramozzino, N.; Vidic, J. Recent Advances in Electrochemical Biosensors for Food Control. *Micromachines* **2023**, *14* (7), 1412.
(50) Marin, M.; Rizzotto, F.; Léguillier, V.; Péchoux, C.; Borezee-Durant, E.; Vidic, J. Naked-eye detection of Staphylococcus aureus in powdered milk and infant formula using gold nanoparticles. *J. Microbiol. Methods* **2022**, *201*, 106578.
(51) White, R. J.; Phares, N.; Lubin, A. A.; Xiao, Y.; Plaxco, K. W. Optimization of electrochemical aptamer-based sensors via optimization of probe packing density and surface chemistry. *Langmuir* **2008**, *24* (18), 10513−10518.

https://doi.org/10.1021/acsomega.3c08219
ACS Omega 2024, 9, 2841−2849